Journal of
Mechanics of
Materials and Structures

RESEARCH ON ACCUMULATIVE PLASTIC DAMAGE FOR LOW-CYCLE FATIGUE ANALYSIS OF HULL NOTCHED PLATE

Junlin Deng, Ping Yang, Yuan Chen and Jin Han

Volume 13, No. 1 January 2018

msp

JOURNAL OF MECHANICS OF MATERIALS AND STRUCTURES
Vol. 13, No. 1, 2018
dx.doi.org/10.2140/jomms.2018.13.121

RESEARCH ON ACCUMULATIVE PLASTIC DAMAGE FOR LOW-CYCLE FATIGUE ANALYSIS OF HULL NOTCHED PLATE

JUNLIN DENG, PING YANG, YUAN CHEN AND JIN HAN

Ship plates suffer from both low-cycle fatigue damage and accumulative plastic damage under asymmetric low-cycle fatigue loading. The accumulative plastic damage under asymmetric low-cycle fatigue loading was investigated using the Chaboche model for numerical analysis, during which the accumulative plastic deformation localized around the region of the notch root was taken as the control parameter. The corresponding experiments were conducted and compared with the results of theoretical analysis in this paper. Based on a series of calculations by finite element simulation, the influence of stress amplitude, mean stress, stress ratio, and initial notch radius on the accumulative plastic strain were investigated and discussed. Based on the fatigue fracture toughness at the root of the ship plate, this paper presents a new assessment approach for additional damage caused by plastic deformation under asymmetrical low cycles.

A list of symbols can be found on page 137.

1. Introduction

Ship hull structures suffer from cyclic loading in navigation conditions, and the phenomenon of accumulative plastic deformation can happen in the ship's structural material under large asymmetric cyclic loads with nonzero mean stress, and as a result, damage to the hull structure will occur [Fukumoto and Kusama 1985; Fujita et al. 1984; Yao and Nikolov 1990]. This kind of damage is called accumulative plastic damage. In fact, a ship's plate under asymmetric low-cycle fatigue loading will produce gradual cumulative damage comprising inelastic deformation and low-cycle fatigue damage.

Accumulative plastic damage is caused by a load that exceeds the tensile ultimate stress or critical compression stress of the plate panels. Fukumoto and Kusama [1985] pointed out that maritime ships should withstand not only static loads but also alternating loads due to the waves encountered during a voyage, and if the alternating loads are large enough, the form of the structural damage to a ship comprises the accumulative plastic damage. The increasing plastic deformation would appear after each load cycle. While the plastic deformation is small in each cycle, it will increase gradually until it reaches the limits of the ductility of the hull steel, which leads to a loss of material ductility and then destruction. According to analysis of the accident on the Japanese ship, the "Onomichi Maru", Fujita et al. [1984] reviewed the problem of accumulative plastic damage around the hull structure, and thought the ship's accident was a typical case of accumulative plastic damage. Yao and Nikolov [1990] also pointed out that the hull structure under large enough alternating loads would undergo buckling or yield failure, resulting in a decrease in the load-bearing capacity of the ship's hull, and consequently leading to overall

Ping Yang is the corresponding author.
Keywords: low cycle fatigue load, notched plate, Chaboche kinematic hardening model, accumulative plastic damage.

fracture failure of the hull structure. In order to prevent a fracture failure caused by accumulative plastic deformation, it is necessary to investigate the accumulative plastic damage of the hull structure caused by asymmetrical loading cycles. Moreover, the existing researches have shown that accumulative plastic deformation has a significant influence on the low-cycle fatigue strength of structural materials under a stress cycle [Lim et al. 2009; Kang et al. 2008], and a coupling interaction in the structural materials between accumulative plastic damage and low-cycle fatigue damage exists. Therefore, it is necessary to study the accumulative plastic damage subjected to low-cycle fatigue loading for ship hull structures in depth.

Studies [Taleb 2013; Hassan and Kyriakides 1994] have shown that the accumulative plastic behavior of structural materials clearly depends on the characteristics of cyclic deformation. Under asymmetric stress loading cycles, the stress-strain curve is not closed, and the plastic strain gradually accumulates. A cumulative plastic damage of the structural materials will occur, which is also called the ratcheting effect. This is one of the most important phenomena of plastic deformation, occurring when the structural materials are subjected to asymmetric stress loading cycles [Hassan and Kyriakides 1994]. It was found that different structural materials exhibit different accumulative plastic behaviors according to test reports on 1070 steel [Jiang and Huseyin 1994] and 1045 steel [Jixi and Jiang 2005].

In addition to experimental studies on accumulative plastic damage, the cyclic constitutive model, which has been widely used to describe the ratcheting effect, is mainly based on the A–F nonlinear kinematic hardening model [Armstrong and Frederiek 1968]. It was developed and improved by Chaboche [1989b], Ohno [1990], and Jiang and Sehitoglu [1996]. Chen et al. [2009] analyzed the mean stress, stress amplitude, and load history on the impact of the HNS ratcheting effect and found that the material had a very strong memory in multistep loading. Kang et al. [2006] studied SS304 stainless steel and found the generation of accumulated plastic strain makes the low-cycle fatigue life of the structural materials decline, and mean stress, stress amplitude, and stress ratio play an important role in the low-cycle fatigue life. Tyfour and Kapoor [1995] indicated that steel under a nonsymmetric stress cycle would have an accumulative incremental deformation, which can cause the loss of steel ductility and material stiffness, and finally result in crack initiation when the accumulated plastic strain reaches a critical value.

However, the existing studies on accumulative plastic failure are almost all confined to material properties, or in a way to conduct research on the fatigue crack initiation of notched specimens. For example, Li et al. [2015] proposed an approach for predicting fatigue crack initiation of a notched specimen with polycrystalline materials through CPFE simulations. In this approach, a CPFE simulation was performed to identify the weakest site and to determine the energy efficiency factor to easily capture the strain inhomogeneity of individual grains. Payne et al. [2010a; 2010b] observed on a notched specimen with an aluminum alloy (AA) 7075 that the initiation of a fatigue crack is significantly influenced by the local deformation, and they emphasized the important role of accumulated plastic deformation near the notch root in fatigue crack initiation. Ranganathan et al. [2011] proposed a short crack approach to determine the fatigue crack initiation life at the notch tip and then they gave acceptable predictions compared with the experiments. There is little research focusing on accumulative plastic damage of notched plate specimens under asymmetrical stress loading cycles.

Therefore, based on experiments on a ship's notched plate, a theoretical analysis of accumulative plastic damage was conducted, and the effect of mean stress and stress amplitude were analyzed by numerical simulation.

2. Theoretical analysis

2.1. ***Plastic strain field at the notch root of a notched plate.*** Under low-cycle fatigue loading, since the plastic deformation is the main part, the elastic strain can be omitted in the actual calculation. Then the stress-strain relationship of the notched plate in an $(n+1)$ cycle's load cycle can be expressed as [Deng et al. 2016]:

$$\begin{aligned}
\Delta\sigma_{eq(n+1)} &= \sqrt{(\Delta\sigma^p_{x(n+1)})^2 - \Delta\sigma^p_{x(n+1)}\Delta\sigma^p_{y(n+1)} + (\Delta\sigma^p_{y(n+1)})^2},\\
\Delta\varepsilon^p_{x(n+1)} &= \frac{f(\Delta\sigma_{eq(n+1)})}{\Delta\sigma_{eq(n+1)}}\big(\Delta\sigma^p_{x(n+1)} - \tfrac{1}{2}\Delta\sigma^p_{y(n+1)}\big),\\
\Delta\varepsilon^p_{y(n+1)} &= \frac{f(\Delta\sigma_{eq(n+1)})}{\Delta\sigma_{eq(n+1)}}\big(\Delta\sigma^p_{y(n+1)} - \tfrac{1}{2}\Delta\sigma^p_{x(n+1)}\big),\\
f(\Delta\sigma_{eq(n+1)}) &= \left(\frac{\Delta\sigma_{eq(n+1)}}{K'}\right)^{1/n'},
\end{aligned} \tag{1}$$

where $\Delta\sigma^p_{x(n+1)}$, $\Delta\sigma^p_{y(n+1)}$, $\Delta\varepsilon^p_{x(n+1)}$, $\Delta\varepsilon^p_{y(n+1)}$ are the local plastic stress and strain at the notch area, n' is the material cyclic hardening coefficient, and K' is the cyclic strength coefficient.

The ship's hull plate is generally under a plane stress state, and the elasto-plastic stress-strain constitutive relation of the notch root is obtained by the stress-strain curve combined with elasticity and plasticity theory. Under low-cycle fatigue loading, combined with the Hencky degeneration equation, the equation can be expressed using an amplitude form as follows [Deng et al. 2017]:

$$\Delta\varepsilon_{ij} = \frac{1+\nu}{E}\Delta\sigma_{ij} - \frac{\nu}{E}\Delta\sigma_{kk}\delta_{ij} + \frac{3}{2}\frac{2f(\Delta\sigma_{eq}/2)}{\Delta\sigma_{eq}}S_{ij}, \tag{2}$$

where

$$\begin{aligned}
&\Delta\sigma_{ij} = (\sigma_{ij})_{\max} - (\sigma_{ij})_{\min}, \quad \Delta\varepsilon_{ij} = (\varepsilon_{ij})_{\max} - (\varepsilon_{ij})_{\min},\\
&\Delta S_{ij} = \Delta\sigma_{ij} - \tfrac{1}{3}\Delta\sigma_{kk}\delta_{ij}, \qquad \Delta\sigma_{eq} = \sqrt{\tfrac{3}{2}\Delta S_{ij}\Delta S_{ij}},
\end{aligned}$$

where ν is Poisson's ratio, E is the elastic modulus, ε_{ij} is the strain component, σ_{ij} is the stress component, ε^p_{ij} is the equivalent plastic strain, σ_{eq} is the equivalent stress, and S_{ij} is the stress deviator.

2.2. ***Accumulated incremental plastic strain at the notch root of a notched plate.*** The basic form of the Chaboche model can be determined according to the literature [Chaboche 1989a; Tong et al. 2013]. Because the strain fatigue of the notched plate under cyclic loading is the main subject under discussion in the paper, the elastic strain can be ignored to focus on the plastic strain problem.

Adopting the Chaboche model [1989a] for the material, the yield function is

$$f_1(\sigma, \chi, R_0, k) = J(\sigma - \chi) - R_0 - k \le 0, \tag{3}$$

where χ is the nonlinear kinematic hardening variable, R_0 is the isotropic hardening variable, k is the yield surface of the initial radius, J is the deviatoric stress space in the von Mises distance, and

$$J(\sigma - \chi) = \sqrt{\tfrac{3}{2}(\sigma' - \chi') : (\sigma' - \chi')}, \tag{4}$$

where σ' and χ' are, respectively, the deviators of σ and χ.

The plastic flow conditions are

$$f_1 = 0 \quad \text{and} \quad \frac{\partial f_1}{\partial \sigma} : \dot{\sigma} > 0. \tag{5}$$

The nonlinear kinematic hardening χ and isotropic hardening variable R_0 can be expressed as:

$$\begin{aligned} \dot{\chi} &= \dot{\chi}_1 + \dot{\chi}_2, & \dot{\chi}_1 &= C_1(a_1\dot{\varepsilon}_p - \chi_1\dot{\varepsilon}_p), \\ \dot{R}_0 &= b(Q - R_0)\dot{\varepsilon}_p, & \dot{\chi}_2 &= C_2(a_2\dot{\varepsilon}_p - \chi_2\dot{\varepsilon}_p), \end{aligned} \tag{6}$$

where C_1, a_1, C_2, a_2, Q, b are material constants, and they are determined by experiment; $\dot{\varepsilon}_p$ is the accumulative plastic strain rate.

According to the study discussing the Chaboche model [Tong et al. 2013], from the differential relationship between the plastic strain and the accumulated plastic strain, the accumulative plastic strain at the notch root of the notch plate in the $(n+1)$ cycle can be

$$d\varepsilon_{p,n+1} = \left\langle \frac{f_1}{Z} \right\rangle^n = \sqrt{\tfrac{2}{3} d\varepsilon^p_{n+1} : d\varepsilon^p_{n+1}}. \tag{7}$$

Here, $d\varepsilon^p_{n+1}$ is the equivalent plastic strain increment at the notch root of the notch plate after the first $n+1$ load cycle, which can be obtained through the Newton–Raphson iteration by the stress-strain relationship (1) of the notch plate in the $n+1$ load cycle.

Substituting (1) and (7) into the Newton–Raphson iteration as in [Budiansky and Hutchinson 1978], the plastic strain increment at the notch root of the notched plate $d\varepsilon^p_{n+1}$ after the $n+1$ cycle can be obtained. In addition, the corresponding incremental plastic strain increment can be obtained too; update the corresponding parameters in turn, and the corresponding incremental plastic strain increment can be obtained for the i-th cycle.

The notched plates are only subjected to uniaxial loading cycles in this paper; therefore, we can obtain the accumulated plastic strain increments after the $N+1$ cycle under uniaxial cyclic loading as

$$\Delta\varepsilon_{p,n+1} = \sum_{i=1}^{n+1} d\varepsilon_{p,n+1} = \sum_{i}^{n+1} \left\langle \frac{f_1}{Z} \right\rangle^n = \sum_{i}^{n+1} \sqrt{\tfrac{2}{3} d\varepsilon^p_i : d\varepsilon^p_i}. \tag{8}$$

Equation (8) is the expression for the value of the accumulated incremental plastic strain at the notch root of the notch plate after an $n+1$ cycle.

2.3. ***The stiffness matrix variation of the notch root region.*** Assuming that all the variables in step n and the strain increment in step $n+1$ are known, the stress increment in step $n+1$ can be obtained by the Newton–Raphson iteration. At the beginning, assume that the incremental plastic strain can be ignored, so the stress in $n+1$ step can be written by the generalized Hooke's law as

$$\sigma^{\mathrm{tr}}_{n+1} = D^e : (\varepsilon_{n+1} - \varepsilon^p_n), \tag{9}$$

where σ is a second-order Cauchy stress tensor and D^e is a fourth-order isotropic elastic tensor.

With the Bauschinger effect (the move of the yield surface center) and the evolution equation of the nonlinear kinematic hardening rate of the structural materials [Jerome et al. 1983], the back stress in the

$n+1$ step is

$$\alpha_{n+1} = \sum_{k=1}^{M} \theta_{n+1}^{k} (\alpha_n^{(k)} + C_k a_k \Delta\varepsilon_{n+1}^{p}), \tag{10}$$

where $\theta_{n+1}^{k} = 1/(1 + C_k \Delta p_{n+1})$, $0 \le \theta_{n+1}^{k} \le 1$; a_k and C_k are material constants which describe the material hardening properties, and M represents the number of back stress force components.

After finding out δ_{n+1}, ε_{n+1}, ε_{n+1}^{p} and other variables at the $n+1$ cycle, the differential equation of the constitutive equation can be pushed to the stiffness matrix of the current moment. According to (9), differential equations can be obtained as follows:

$$d\Delta\delta_{n+1} = D^e : (d\Delta\varepsilon_{n+1} - d\Delta\varepsilon_{n+1}^{p}). \tag{11}$$

By differential calculation, (12) can be obtained as follows:

$$d\Delta\varepsilon_{n+1}^{p} = L_{n+1}^{-1} : J_{n+1}^{0} : 2GI_d : d\Delta\varepsilon_{n+1}, \tag{12}$$

where

$$L_{n+1} = n_{n+1} \otimes n_{n+1} - J_{n+1}^{0} : H_{n+1}; \qquad J_{n+1}^{0} = \sqrt{\tfrac{3}{2}}\Delta p_{n+1} J_{n+1},$$

$$H_{n+1} = \left(2G + \sum_{k=1}^{m} \theta_{n+1}^{k} C_k \alpha_k\right) I - n_{n+1} \otimes \left(\frac{2}{3} \sum_{k=1}^{m} C_k \theta_{n+1}^{(k)} \alpha_{n+1}^{(k)}\right), \qquad I_d = I - \tfrac{1}{3}\delta \otimes \delta.$$

Here, I_d is the fourth-order tensor, and δ is the second-order tensor.

Furthermore, $J_{n+1} = (I - n_{n+1} \otimes n_{n+1})/\|S_{n+1} - \alpha_{n+1}\|$, I is the fourth-order tensor, $I_{ijkl} = \frac{1}{2}(\delta_{ik}\delta_{jl} + \delta_{jk}\delta_{il})$; and $n_{n+1} = (S_{n+1} - \alpha_{n+1})/\|S_{n+1} - \alpha_{n+1}\|$. S_{n+1}, α_{n+1} are the partial stress tensor and back stress tensor, respectively, and p_{n+1} is the equivalent accumulative plastic strain at the notch root in the $n+1$ step.

Finally, substituting (12) into (11), the stiffness matrix of the models is as follows:

$$\frac{d\Delta\delta_{n+1}}{d\Delta\varepsilon_{n+1}} = D^e - 4G^2 (L_{n+1}^{-1} : J_{n+1}^{0}) : I_d. \tag{13}$$

Substituting (13) into (9), the variation of the plastic deformation at the notch root region can be obtained in the $n+1$ cycle because the accumulative plastic deformation stiffness is reduced. Using the Newton–Raphson iteration method, the variation of plastic deformation at the notch root can be obtained in the corresponding cycles.

2.4. ***The accumulated plastic damage life.*** The accumulative plastic strain can produce additional damage in the stress control loop. When the average stress is that of nonzero asymmetrical stress cycles, in order to consider the effect of accumulative plastic strain, the accumulative plastic strain failure cycles can be calculated using the model proposed by [Xia and Kujawki 1996]. Then

$$\sigma_{\max} \dot{\varepsilon}_r^{p} = \kappa_r N_r^{\beta}. \tag{14}$$

Then

$$N_r = \left(\frac{\sigma_{\max} \dot{\varepsilon}_r^{p}}{\kappa_r}\right)^{1/\beta}, \tag{15}$$

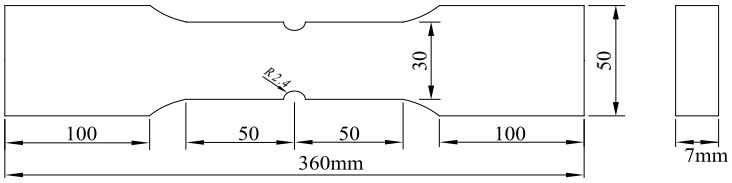

Figure 1. A notched plate specimen (the notch diameter is 4.8 mm, thickness is 7 mm).

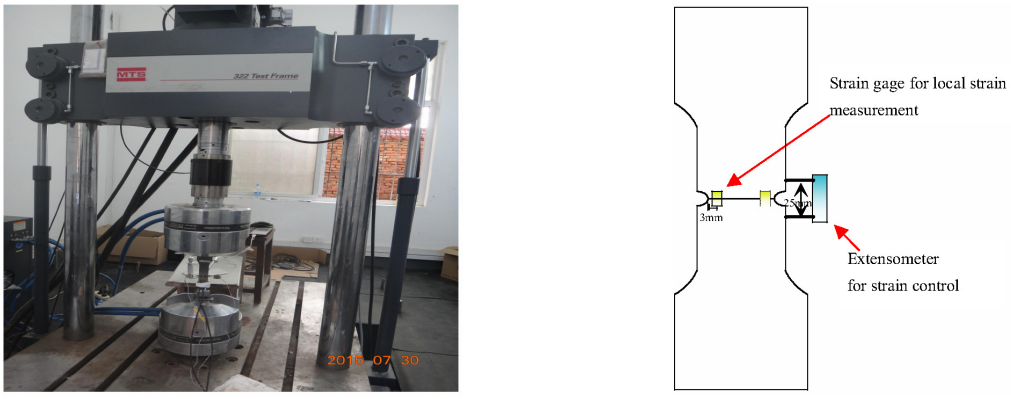

Figure 2. Testing rigs and the locations of the strain gage and extensometer for strain measurements.

where ε_r^p is the accumulative plastic strain, $\dot{\varepsilon}_r = d\varepsilon_r^p/dN$, which is obtained by (8), is the accumulative plastic strain rate when the accumulative plastic strain steadily develops, and κ_r, β are the corresponding material constants, which are obtained by fitting the experimental measurements.

Equation (15) is the expression for the value of the accumulated plastic damage life of the hull notched plate.

3. Experimental investigations

3.1. ***Experimental setup.*** In order to investigate the local cumulative plastic damage characteristics of the hull notched plate under asymmetric stress loading cycles, a series of experiments were carried out and the properties of the materials studied. The accumulative plastic damage experiments were conducted on a 7 mm thick hull, and notched plate specimens with other dimensions as shown in Figure 1. The tests were performed in air and at room temperature using a computer-controlled MTS322 servo-hydraulic testing machine. The MTS fatigue testing machine and data processing program were used in the tests. The specimen and the test setup are shown in Figure 2.

The Q235 steel is low carbon steel, which is widely used in hull structures. It was employed in the tests where the uniaxial tensile stress-strain curve of the steel was obtained by tensile tests as shown in Figure 3. The basic material and mechanical properties of the Q235 steel were obtained by tensile tests as shown in Table 1. The chemical composition (in % wt) of this material is C-0.17; Mn-0.49; Si-0.23; P-0.026; and Si-0.025. Sinusoidal loading with stress control was adopted in the tests. A 0.25 Hz frequency was chosen based on other low-cycle fatigue test results available in the literature.

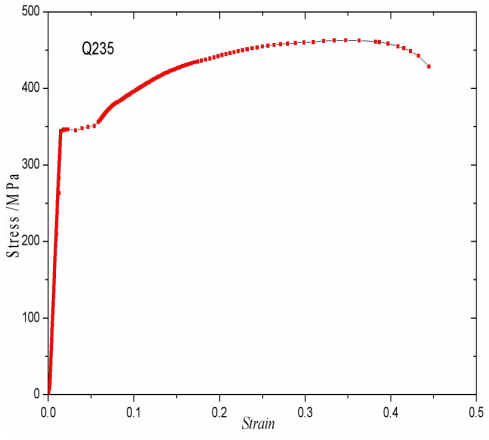

Figure 3. The uniaxial tensile stress-strain curve.

The notched plate specimens were subjected to stress- or strain-controlled fully reversed low-cycle fatigue loading. In the strain-controlled test, the strain range measured by an extensometer attached at the back face was controlled so that it kept the objective value. The extensometer had a 25 mm gage length, and ± 1 mm range, in order to reduce the influence of the notch geometry on the strain measurement, and a 0.01% extensometer strain control accuracy whose operating temperature range was $-80\,^{\circ}\mathrm{C}$ to $200\,^{\circ}\mathrm{C}$. The accumulative plastic strain at the notched root region was simultaneously measured by a strain gage attached 3 mm away from the notch root as shown in Figure 2. The strain range measured by the strain gage was referred to as the accumulative plastic strain at the notch root and used for (15) to calculate the accumulative plastic damage life of the notched plate specimen.

The tests were conducted under constant amplitude loading with different mean stresses and stress amplitudes to study the effect on the accumulative plastic strain deformation of the hull notched plate. The real-time information such as time, load, and extensometer strain were recorded. After the accumulative plastic failure, fractographs and microscopic changes were examined using a LEO Electron Microscopy 1530 VP field emission scanning electron microscope (FESEM) to analyze the failure mechanisms. The loading conditions and experimental results of the Q235 steel are summarized in Table 2. An example of the appearance of accumulative plastic damage is shown in Figure 4 and the damage morphologies are shown in Figure 5.

3.2. ***Observation of the damage morphology.*** Figure 4 shows an example of the appearance of accumulative plastic damage at the notched root region of the specimen from Q235 steel inspected during an accumulative plastic damage test with a stress amplitude of $\sigma_a = 260$ MPa and mean stress of $\sigma_m = 60$ MPa. Observation of the notched root region in the test did detect the corresponding plastic deformation phenomenon at the notched root region under low-cycle fatigue loading.

Figure 5 shows examples of the accumulative plastic damage morphology of the notched plate of Q235 steel under the stress loading cycle with the same mean stress of $\sigma_m = 60$ MPa, where the stress amplitude (σ_a) was 240 MPa in No. 1; 260 MPa in No. 2, and 280 MPa in No. 3. An observation of the notch root region in the test detected the corresponding plastic deformation phenomenon under the fatigue loading stress cycle with the same mean stress of $\sigma_m = 60$ MPa. There was an obvious plastic

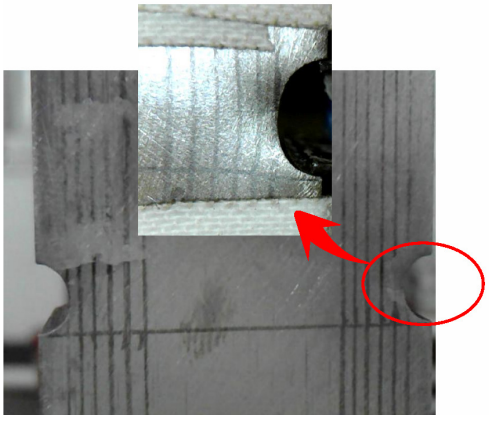

Figure 4. Accumulative plastic damage morphology of the notched plate specimen.

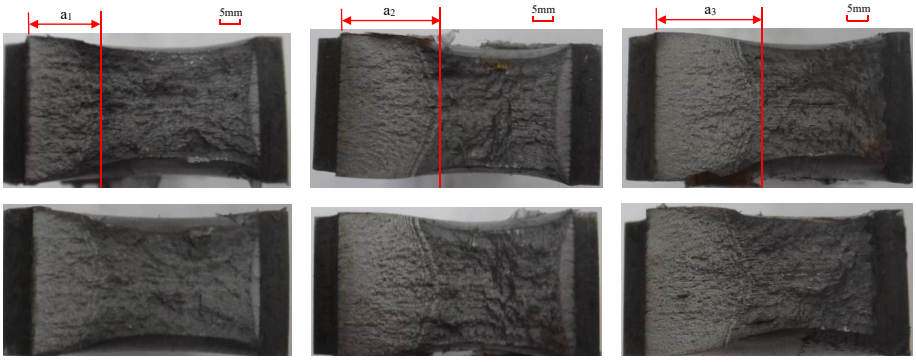

Figure 5. Accumulative plastic damage morphology of the notched plate specimens: No. 1 (left column); No. 2 (middle column); No. 3 (right column).

deformation at the root region of the specimen after the low-cycle fatigue loading. The tests showed that the irregularity on the fracture surface was more significant in the accumulative plastic damage test with the constant mean stress but gradual increase in stress amplitude. The fracture morphologies show obvious accumulative plastic damage and a transgranular fracture. It can be found that the accumulation of plastic deformation at the notch root is obvious in the case of higher stress amplitude. Greater plastic damage was produced in the asymmetric stress loading-cycle process, which led to a decrease in the ability to resist deformation of the material. With the increase in stress amplitude, a larger accumulative plastic deformation will lead to earlier fracture failure.

Therefore, it is necessary to consider the effect of accumulative plastic damage in low-cycle fatigue problems under asymmetric stress loading cycles.

3.3. ***Experimental result and discussion.*** The stress-strain curve of Q235 steel based on experiments under uniaxial tensile loads is shown in Figure 3. The Q235 steel sample mechanical performance parameters were obtained according to the MTS fatigue testing machine data collection system and

material	E (GPa)	K (MPa)	σ_y (MPa)	σ_b (MPa)
Q235	206	1193	310	475

Table 1. The mechanical properties of Q235.

stress amplitude (MPa)	specimen number	mean stress (MPa)	accumulated plastic damage life (N)
240	No. 01	0	2667
	No. 02	20	2376
	No. 03	40	2212
	No. 04	60	2024
260	No. 05	0	2435
	No. 06	20	2168
	No. 07	40	1800
	No. 08	60	1971
280	No. 09	0	2530
	No. 10	20	2329
	No. 11	40	1875
	No. 12	60	1147

Table 2. Accumulated plastic damage life at the notched root for Q235 steel.

numerical fitting with Origin software based on a static load in the tensile test results. The parameters are shown in Table 1.

The specimens were tested for stress amplitude ($\sigma_a = 240$ MPa, 260 MPa, 280 MPa) and mean stress ($\sigma_m = 0$ MPa, 20 MPa, 40 MPa, 60 MPa) under asymmetrical stress loading cycles. According to the strain gage, which is arranged at the notched root of the specimen, the accumulative plastic damage life of the notched plate under asymmetrical cyclic loading is shown in Table 2.

Since it is known that if the mean stress is larger, the notched root mainly appears with accumulative plastic damage under asymmetrical cyclic loading, the mean stress (which is relatively large in Table 2) was chosen to be combined with (14) for fitting the Q235 steel material parameters. The corresponding results are listed in Table 3.

When the mean stress is large enough, the accumulative plastic damage may primarily be produced at the notch root under the asymmetrical stress cyclic loading [Kang et al. 2002]; therefore, the specimens with relatively higher mean stresses, as shown in Table 2, were chosen for numerical fitting. Combined with the selected experimental results in Table 3 and the material parameters, the numerical fitting was performed for (8), and the parameter values of $K_r = 200.83$ and $\beta = -1.37$ were obtained.

4. Numerical analysis and discussion

In the present study, the commercial finite element software ANSYS was employed, and in the material model, the von Mises yield function, associated flow rule, and Chaboche kinematic hardening model

stress amplitude	mean stress	specimen number	accumulative plastic damage life (N)	accumulative plastic rates ($\dot{\varepsilon}_r$)
240	60	No. 04	2024	0.0011
260	60	No. 08	1971	0.0019
280	60	No. 12	1147	0.0036
280	40	No. 11	1875	0.0029
280	20	No. 10	2329	0.0014

Table 3. Loading conditions and experimental results for Q235 steel.

E (Gpa)	ν	Q	b	k	–
206	0.3	162	8.5	145	–
C_1	α_1	C_2	α_2	C_3	α_3
140000	8750	75000	238	1950	0

Table 4. Values for the material parameters of Q235 steel for a viscoplastic constitutive material model.

were used. The Chaboche kinematic hardening model is an advanced material model that is capable of capturing basic cyclic plastic responses of materials such as the Bauschinger effect, plastic shakedown, ratcheting resulting from asymmetric stress cycles, and mean stress relaxation resulting from asymmetric strain cycles. The constitutive equations contain 11 material parameters, namely, E, ν, k, b, Q, C_1, α_1, C_2, α_2, C_3, α_3. The kinematic hardening behavior is described by C_1, α_1, C_2, α_2, C_3, and α_3, where α_1, α_2, and α_3 are the saturated values of the kinematic hardening variables, and C_1, C_2, and C_3 indicate the speed with which the saturation is reached. The isotropic hardening is depicted by Q and b, the initial size of the yield surface is represented as k, E is the Young's modulus, and ν is Poisson's ratio. The parameter values, optimized from the uniaxial test data of Q235 at room temperature, are listed in Table 4. The above material model is adopted in the finite element software ANSYS. Comparisons of the experimental result and the model simulations are given in Figure 6 for the stress-controlled cyclic test.

A notched plate specimen was considered and the finite element meshes for the specimen are shown in Figure 7. Moreover, the APDL language was adopted to establish the finite element model in order to improve the data processing efficiency. Because of the thin thickness and loading conditions, finite element modeling of the notched plate specimen was treated as a plane stress case. Due to the symmetry, only a quarter of the specimen was considered. The plane 182 element type in ANSYS was used in the FE mesh model. To simulate the high stress and strain gradients, refined mesh elements were used for the region near the notch root. The element size in the notch root region was chosen as 0.05 mm to obtain a relatively high accurate stress-strain response.

4.1. ***Stress-strain curve at the notched root of specimen.*** Finite element computations were carried out on the hull notched plate specimen to study the detailed accumulative plastic deformation response. For consistency within the experiment, the same loading condition was adopted in the numerical model. With the sinusoidal cyclic loads applied on the quarter of the finite element model in Figure 7, combined with the fitting material with the model of coefficients in Table 3 (based on the Chaboche nonlinear

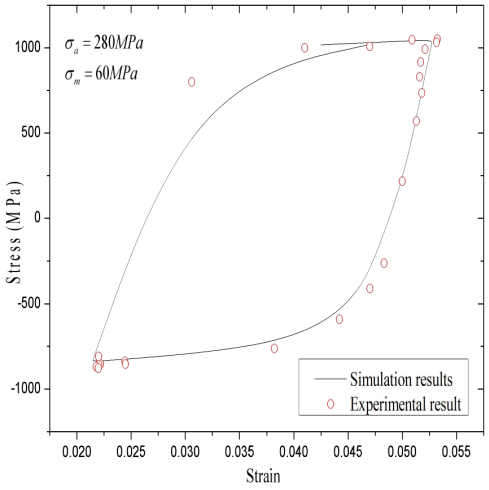

Figure 6. Stress and strain hysteresis loop for the notched plate.

kinematic hardening model), finite element analysis was carried out under low-cycle fatigue loading, and we obtained a stress-strain hysteresis loop at the notched root under asymmetrical stress cycling loads, which is shown in Figure 8.

Finite element computations were carried out for over 40 cycles at the selected asymmetrical stress loading cycles. The normal stress-strain response for mean stress ($\sigma_m = 20$ MPa, 40 MPa, 60 MPa) is shown in Figure 8 for a Gauss integration point just ahead of the notched root. The Gauss integration point is located most closely to the notched root with a polar coordinate of ($r = 3.8\,\mu$m, $\theta = 45°$). The stress-strain response exhibits a progressive shift in the direction of increasing tensile strain, a phenomenon known as ratcheting, which means the plastic strain clearly accumulates at the notched root under asymmetrical stress loading cycles, but also no obvious mean stress relaxation is observed from Figure 8. After several loading cycles, the accumulative plastic strain rate tends to be insignificant, which means that the stabilized stress-strain responses are reached. Figure 8 shows that with a plate undergoing asymmetrical stress loading cycles, the notched root appeared with the accumulation of plastic strain, the accumulating growth of initial plastic deformation increases faster, and then it gradually reduces and tends to be stable. What can be seen from the figure is that the stress-strain hysteresis loop of Q235 steel does not change significantly in shape, which is obviously different from [Kang et al. 2002], which reported that the stress-strain hysteresis loop of cyclic softening materials gradually increases.

The peak cyclic loading case with the stress amplitude of 280 MPa and mean stress of 60 MPa were, respectively, applied to the finite element model. The stress and strain contours are obtained, respectively, as shown in Figure 9. It can be seen in Figure 9 that the stress at the notch root of the notched plate specimen is obviously higher than the yield stress. The plastic deformation is relatively large.

Combined with Figure 8, it can be observed that the plastic deformation clearly accumulates with the increase in the cyclic numbers under asymmetric loading cycles. In the initial cycles, the accumulated plastic strain increments grow rapidly with the increasing number of cycles; the accumulated plastic strain increment rate is gradually decreased, and then becomes stable. Therefore, the additional damage caused

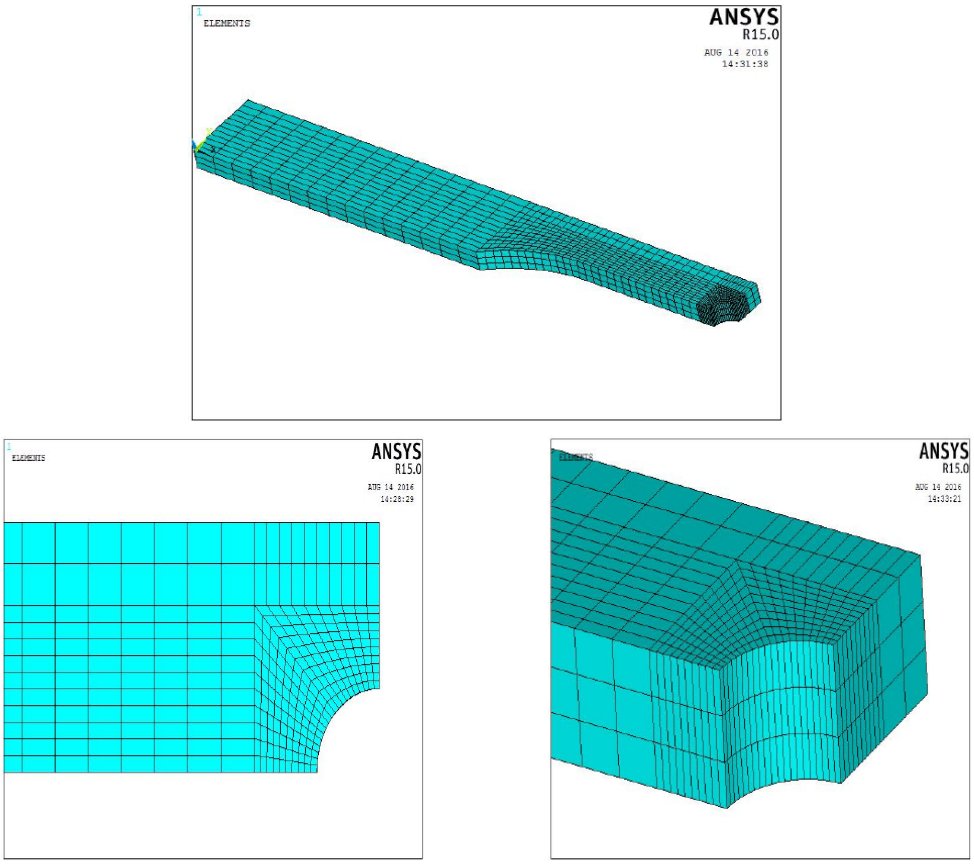

Figure 7. A quarter of the finite element model for the notched plate specimen and the refined mesh for the notch root.

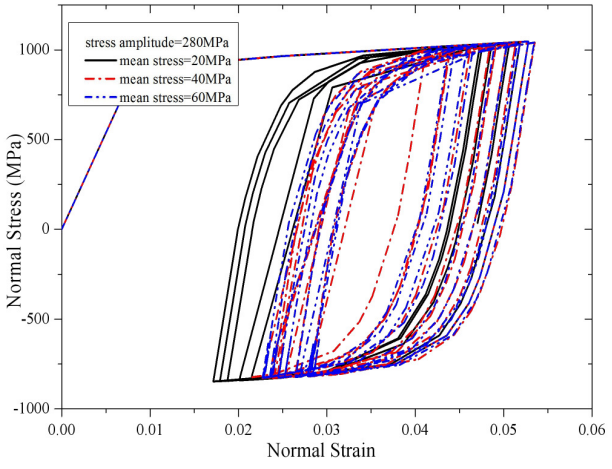

Figure 8. The stress-strain curve at the root of the notched plate.

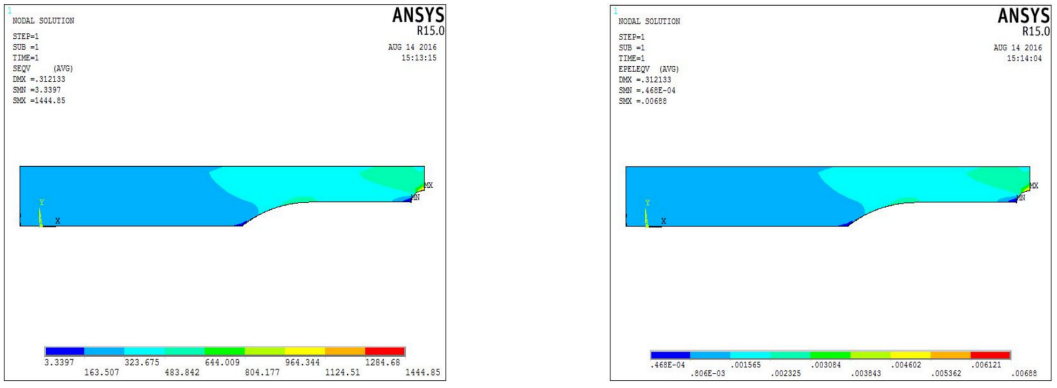

Figure 9. The stress and strain contours under the 280 MPa stress amplitude and 60 MPa mean stress of the peak cyclic loading case: Stress contour (left); Strain contour (right).

by plastic deformation should be considered when evaluating fracture toughness under asymmetric low-cycle fatigue cyclic loading.

In the present work, the accumulative plastic strain is examined and the results are plotted against the number of cycles as shown in Figures 10 and 11, left. Obviously the accumulative plastic strain increases with the increase in the stress ratio for a given stress amplitude. The results determined that the stress-strain response near the notched root remains fairly constant during the cyclic loading, and the accumulative plastic strain increases with the increase in mean stress. The continuous increase in accumulative plastic strain may eventually lead to a material separation near the notched root, and hence crack initiation and propagation.

4.2. ***The effect of mean stress and stress amplitude.*** As shown in Figure 10, left, the results from the

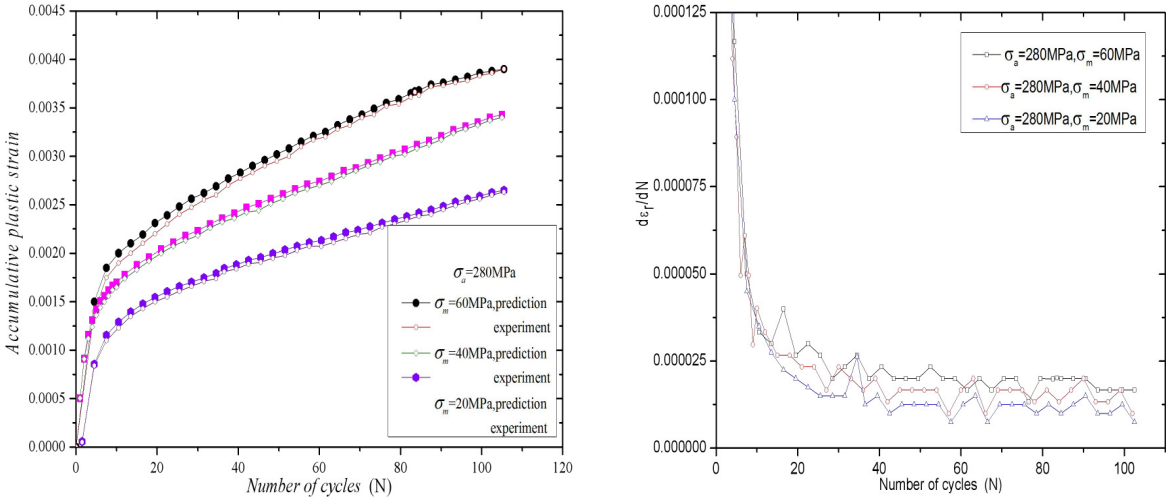

Figure 10. Accumulative plastic strains (left) and strain rates (right) versus cyclic numbers for different mean stresses.

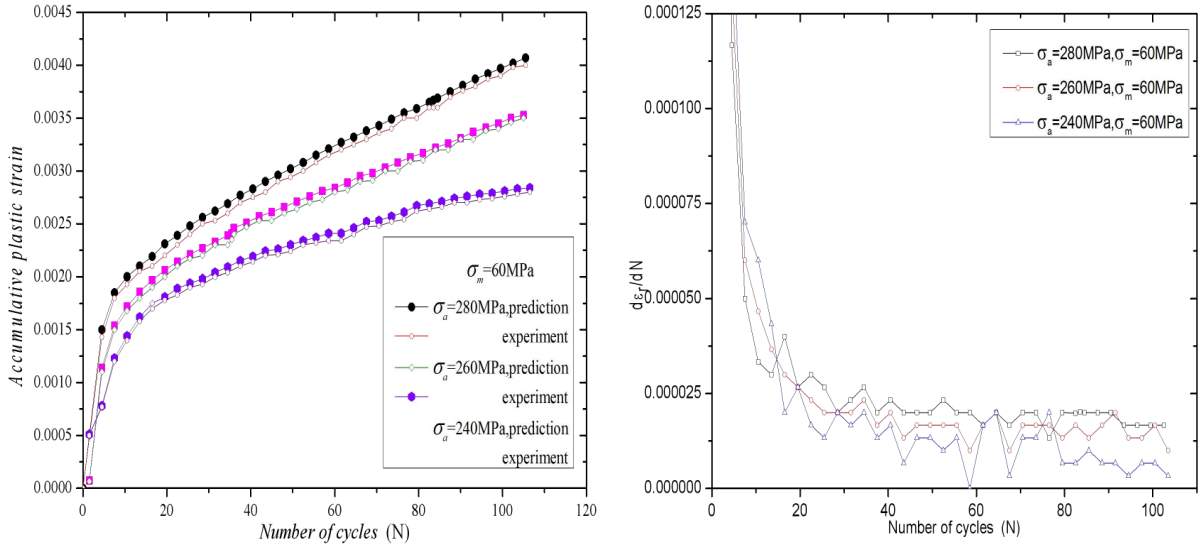

Figure 11. Accumulative plastic strains (left) and strain rates (right) versus cyclic numbers for different stress amplitudes.

predictive model obviously agree well with the experiments. Due to the existence of the mean stress, the notch root of the hull notched plate has an accumulated incremental plastic deformation in the mean stress direction. The accumulated incremental plastic deformation accumulates quickly in the initial stage, and the mean stress is bigger; the accumulative plastic deformation is also relatively larger, and as the accumulated incremental plastic deformation increases, the accumulated incremental plastic deformation rate at the notch root of the hull notched plate specimen decreases gradually and tends to a nonzero constant steady state in Figure 10, right. These trend results are basically the same as in [Satyadevi et al. 2007].

As shown in Figure 11, left, the results from the predictive model obviously agree well with the experiments. Under the same mean stress and different stress amplitude cyclic loadings, the notch root of accumulated plastic strain gradually increased with the increase in stress amplitude. When the stress amplitude is larger, the accumulated incremental plastic deformation is also relatively larger, and the stress amplitude is higher, and the material quickly progresses into the accumulated incremental plastic deformation stage. The trend in this kind of change is similar to that of [Paul et al. 2010]. Due to the existence of the stress amplitude, the accumulated incremental plastic damage occurred in the axial direction of the notched specimen. The accumulated incremental plastic deformation of the notch root is quickly accumulated in the initial cycle, and the rate of plastic change tends to be a nonzero constant.

Finally, according to the test results and the calculation results of Figures 10 and 11, right, the accumulative plastic damage values at the notch root are solved by selecting the accumulative plastic deformation rate curve at a stable level under asymmetric low-cycle fatigue loading.

4.3. ***Accumulative plastic damage life.*** Considering the accumulative plastic damage effect, the accumulative plastic damage life of a notched plate should be analyzed under asymmetrical stress loading cycles; this paper predicts numerical results and experimental results; then the calculation results of Neuber's empirical approach [1961] based on the determination of local strain amplitudes in the vicinity

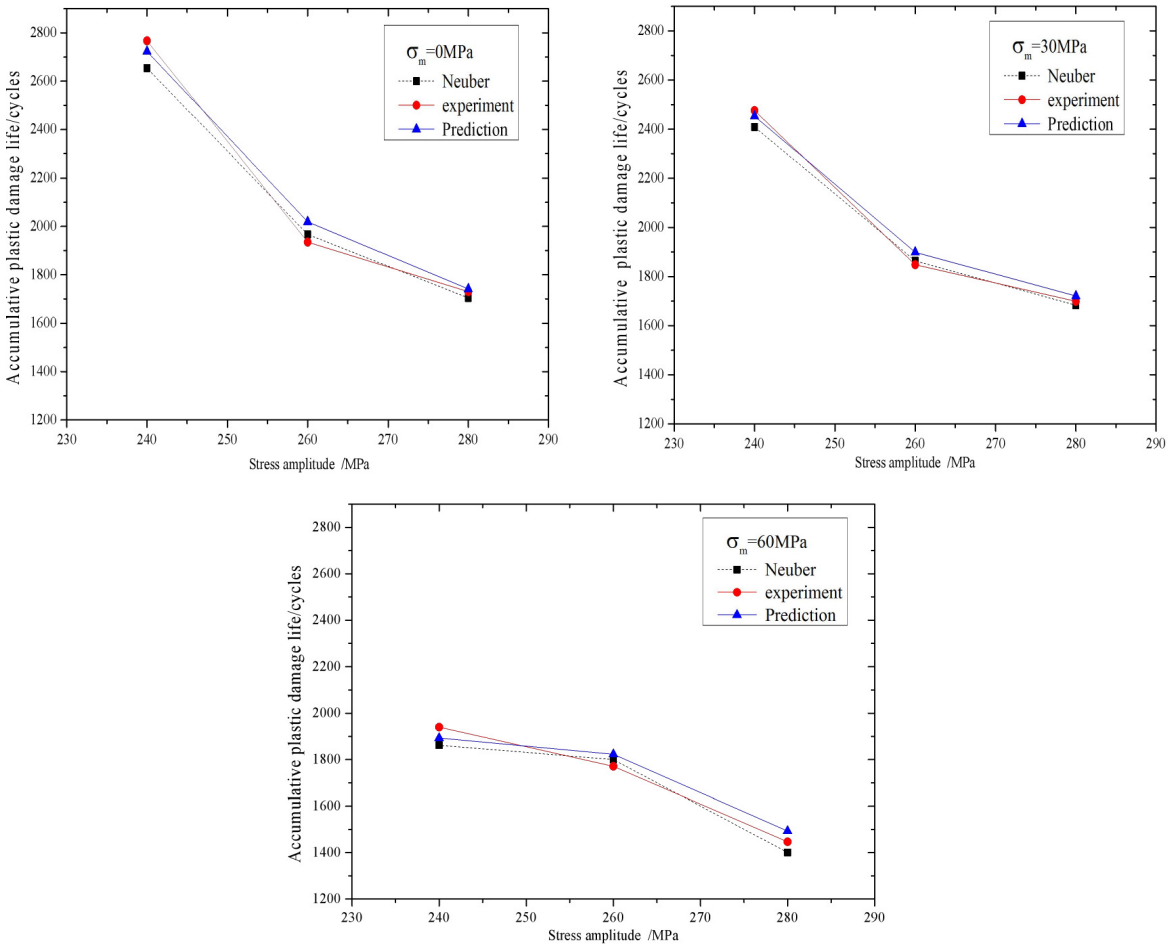

Figure 12. The comparison of prediction models and experimental measurements under different stress amplitudes.

of a notch are compared with the above results. Combined with the first part of the study, under different mean stresses and stress amplitudes, the accumulative plastic damage life of the notched plate are shown in Figure 12.

Figure 12 shows the accumulative plastic damage life of the hull notched plate under the same mean stresses at different stress amplitudes, so the damage life is related to the change in stress amplitude. Figure 11, left, shows that when the stress amplitude is high, the accumulative plastic deformation of the hull notched plate steadily develops, and it will eventually produce large accumulative plastic damage. At the same time, the larger accumulative plastic deformation of the notched root is the main form of the hull notched plate damage. Figure 11, right, shows that the accumulative plastic strain rate increases with the increase of stress amplitude; therefore, the accumulated incremental plastic damage life of the hull notched plate decreases with the increase of stress amplitude. Due to the damage caused by the accumulative plastic damage under the same mean stress, the greater the stress amplitude is, the shorter the accumulative plastic damage life is. The nonzero average stress accumulative plastic failure life of the

specimen is significantly shorter than that with average stress, which is equal to zero. With the increase of stress amplitude, the accumulative plastic damage life is significantly reduced, indicating that under the same average stresses and different stress amplitudes, the accumulative plastic deformation caused by the notch root of the ship's hull is an additional damage, which reduces the accumulative plastic damage life of the hull notched plate.

In addition, to illustrate the relationship between the accumulative plastic damage life and the accumulative plastic strain, (14) is fitted to the experimental data resulting in $K_r = 200.83$ and $\beta = -1.37$ for mean stress and stress amplitude, respectively. From the three respective results, the errors, based on a comparison with the predicted results of accumulative plastic damage life at the hull notched plates, the experimental results, and the Neuber rule, are in the acceptable range. This shows that the prediction model of the fitting parameter K_r and β is capable of forecasting the accumulative plastic damage life of a hull notched plate under low-cycle fatigue asymmetrical stress loading cycles.

5. Conclusion

The accumulative plastic deformation at the notch root of a hull notched plate under asymmetric cyclic loading is theoretically analyzed by adopting the Newton–Raphson iterative method. Through the experiment and finite element simulation, the accumulative plastic damage life of the notched plate under low-cycle fatigue loads is studied and the following conclusions can be drawn:

(1) Combined with the Newton–Raphson iterative method to deduce the accumulative plastic deformation's theoretical solution under low-cycle high-stress asymmetrical cyclic loading, a significant accumulative plastic damage will be produced at the notch root of the hull notched plate under low-cycle fatigue loading, and the accumulative plastic damage depends on mean stress and the stress amplitude of asymmetric cyclic loading. The increase of the accumulative plastic deformation at the notch root is relatively large in the beginning stages, then gradually tends to stabilize.

(2) The theoretical solutions of the tangent stiffness at the notch root of the notched plate are derived. The accumulative plastic deformation at the notch root significantly reduces the tangent stiffness at the notch root, and the decrease of the stiffness of the notch root is further aggravated by the accumulation of plastic deformation. With the increase of the number of cycles, the accumulative plastic deformation at the notched root gradually increases and eventually leads to the depletion of the notched plate material.

(3) The assessment model for the accumulative plastic damage life for the hull notched plate is established under low-cycle fatigue loading, and based on the theoretical analysis and numerical simulation, the results of the relevant model parameters are fitted with the experimental results. Compared to the experimental results, the model can estimate the accumulative plastic damage life of the hull notched plate under low-cycle fatigue loads well.

Acknowledgements. The authors are indebted to the National Natural Science Foundation of China (Grant No. 51479153) and the Provincial Natural Science Foundation of Guangxi for financial support (Grant No. 2016GXNSFAA380033) and the basic ability promotion program for young and middle-aged teacher of University in Guangxi (No. 2017KY0809).

List of symbols

K'	hardening modulus (MPa)	n'	hardening exponent
ν	Poisson's ratio	E	Young's modulus (MPa)
σ	local stress (MPa)	ε	local strain
σ_{ij}	stress component	ε_{ij}	strain component
$\Delta\sigma^p_{x(n+1)}$	x-direction plastic stresses in $n+1$ cycle		
$\Delta\sigma^p_{y(n+1)}$	y-direction plastic stresses in $n+1$ cycle		
$\Delta\varepsilon^p_{x(n+1)}$	x-direction plastic strains in $n+1$ cycle		
$\Delta\varepsilon^p_{y(n+1)}$	y-direction plastic strains in $n+1$ cycle		
σ_{eq}	equivalent stress	ε^p_{eq}	equivalent plastic strain
χ	nonlinear kinematic hardening variable	R_0	isotropic hardening variable
k	yield surface of the initial radius	J	deviatoric stress space in the von Mises distance
S_{ij}	stress deviator	S_{n+1}	partial stress tensor
α_{n+1}	back stress tensor	p_{n+1}	equivalent accumulative plastic strain
D^e	fourth-order isotropic elastic tensor	$\sigma_{\max}$	maximum stress (MPa)
ε^p_r	accumulative plastic strain	$d\varepsilon^p_r/dN$	accumulative plastic strain rate
κ_r	material constant	β	material constant
N_r	accumulative plastic damage life (cycles)		
σ_y	yield stress (MPa)	σ_b	tensile stress (MPa)
σ_n	nominal stress (MPa)	ε_n	nominal strain
ε_a	local strain amplitude	σ_m	effective mean stress (MPa)

References

[Armstrong and Frederiek 1968] P. J. Armstrong and C. O. Frederiek, "A mathematical representation of the multiaxial Bauschinger effect", Report RD/B/N 731, Central Electricity Generating Board, 1968.

[Budiansky and Hutchinson 1978] B. Budiansky and J. W. Hutchinson, "Analysis of crack closure in fatigue crack growth", *J. Appl. Mech.* **45** (1978), 267–276.

[Chaboche 1989a] D. Chaboche, J. L. Nouailhas, "Constitutive modeling of ratchetting effects, part I: Experimental facts and properties of the classical models", *J. Eng. Mater. Technol.* **111**:4 (1989), 384–392.

[Chaboche 1989b] J. L. Chaboche, "Constitutive equations for cyclic plasticity and cyclic viscoplasticity", *Int. J. Plast.* **5** (1989), 247–302.

[Chen et al. 2009] G. Chen, S.-C. Shan, X. Chen, and H. Yuan, "Ratcheting and fatigue properties of the high-nitrogen steel X13CrMnMoN18-14-3 under cyclic loading", *Comput. Mater. Sci.* **46**:3 (2009), 572–578.

[Deng et al. 2016] J. Deng, B. Du, and P. Yang, "Research on the fracture toughness for ship cracked plates based on the accumulative increment plastic deformation", *J. Ship Mech.* **20**:6 (2016), 748–757.

[Deng et al. 2017] J. L. Deng, P. Yang, and Y. Chen, "Low-cycle fatigue crack initiation life of hull-notched plate considering short crack effect and accumulative plastic damage", *Appl. Ocean Res.* **68** (2017), 65–76.

[Fujita et al. 1984] Y. Fujita, T. Nomoto, and K. Yuge, "Behavior of deformation of structural members under compressive and tensile loads (1st report) on the buckling of a column subjected to repeated loading", *J. Soc. Naval Arch Japan* **156** (1984), 346–354.

[Fukumoto and Kusama 1985] Y. Fukumoto and H. Kusama, "Cyclic behaviour of plates under in plane loading", *Eng. Struct.* **7** (1985), 56–63.

[Hassan and Kyriakides 1994] T. Hassan and S. Kyriakides, "Ratcheting of cyclically hardening and softening materials, I: Uniaxial behavior", *Int. J. Plast.* **10**:2 (1994), 149–184.

[Jerome et al. 1983] S. P. Jerome, A. Dinsenbacher, and E. B. Jeffrey, "A method for estimating life time loads and fatigue lives for Swath and conventional monohull ships", *Naval Eng. J.* **95**:3 (1983), 63–85.

[Jiang and Huseyin 1994] Y. Jiang and S. Huseyin, "Cyclic ratcheting of 1070 steel under multiaxial stress states", *Int. J. Plast.* **10** (1994), 608–679.

[Jiang and Sehitoglu 1996] Y. Jiang and H. Sehitoglu, "Modeling of cyclic ratcheting plasticity, part I: Development of constitutive relations", *J. Appl. Mech.* **63** (1996), 720–725.

[Jixi and Jiang 2005] Z. Jixi and Y. Jiang, "An experimental study of inhomogeneous cyclic plastic deformation of 1045 steel under multiaxial cyclic loading", *Int. J. Plast.* **21** (2005), 2174–2190.

[Kang et al. 2002] G. Kang, Q. Gao, L. Cai, and Y. Sun, "Experimental study on the uniaxial and nonproportionally multiaxial of SS304 stainless steel at room and high temperatures", *Unclear Eng. Design* **216** (2002), 13–26.

[Kang et al. 2006] G. Kang, J. Kan, Q. Zhang, and Y. Sun, "Time-dependent ratchetting experiments of SS304 stainless steel", *Int. J. Plast.* **22** (2006), 858–894.

[Kang et al. 2008] G. Kang, Y. Liu, and J. Ding, "Multiaxial ratcheting-fatigue interactions of annealed and tempered 42CrMo steels: experimental observations", *Int. J. Fatigue* **30** (2008), 2104–2118.

[Li et al. 2015] L. Li, L. Shen, and G. Proust, "Fatigue crack initiation life prediction for aluminium alloy 7075 using crystal plasticity finite element simulations", *Mech. Mater.* **81** (2015), 84–93.

[Lim et al. 2009] C. B. Lim, K. S. Kim, and J. B. Seong, "Ratcheting and fatigue behavior of a copper alloy under uniaxial cyclic loading with mean stress", *Int. J. Fatigue* **31**:3 (2009), 501–507.

[Neuber 1961] H. Neuber, "Theory of stress concentration for shear-strained prismatical bodies with arbitrary nonlinear stress-strain law", *J. Appl. Mech.* (*ASME*) **28**:4 (1961), 544–560.

[Ohno 1990] N. Ohno, "Recent topics in constitutive modeling of cyclic plasticity and viscoplasticity", *Appl. Mech. Rev.* **43**:11 (1990), 283–295.

[Paul et al. 2010] S. K. Paul, S. Sivaprasad, and S. Dhar, "Ratcheting and low cycle fatigue behavior of SA333 steel and their life prediction", *J. Nuclear Mater.* **401** (2010), 17–24.

[Payne et al. 2010a] J. Payne, G. Welsh, R. J. Christ Jr., and J. Nardiello, "Observations of fatigue crack initiation in 7075-T651", *Int. J. Fatigue* **32** (2010), 247–255.

[Payne et al. 2010b] J. Payne, G. Welsh, R. J. Christ Jr., J. Nardiello, and J. M. Papazian, "Observations of fatigue crack initiation in 7075-T651", *Int. J. Fatigue* **32** (2010), 247–255.

[Ranganathan et al. 2011] N. Ranganathan, H. Aldroe, F. Lacroix, F. Chalon, R. Leroy, and A. Tougui, "Fatigue crack initiation at a notch", *Int. J. Fatigue* **33** (2011), 492–499.

[Satyadevi et al. 2007] A. Satyadevi, S. M. Sivakumar, and S. S. Bhattacharya, "A new failure criterion for materials exhibiting ratcheting during very low cycle fatigue", *Mater. Sci. Eng. A* **452-453** (2007), 380–385.

[Taleb 2013] L. Taleb, "About the cyclic accumulation of the inelastic strain observed in metals subjected to cyclic stress control", *Int. J. Plast.* **43** (2013), 1–19.

[Tong et al. 2013] J. Tong, L. G. Zhao, and B. Lin, "Ratcheting strain as a driving force for fatigue crack growth", *Int. J. Fatigue* **46** (2013), 49–57.

[Tyfour and Kapoor 1995] W. R. Tyfour and A. Kapoor, "The steady state wear behaviour of pearlitic rail steel under dry rolling-sliding contact conditions", *Wear* **180** (1995), 79–89.

[Xia and Kujawki 1996] Z. Xia and D. Kujawki, "Effect of mean stress and ratcheting strain on fatigue life of steel", *Int. J. Fatigue* **18** (1996), 335–341.

[Yao and Nikolov 1990] T. Yao and P. I. Nikolov, "Buckling/plastic collapse of plates under cyclic loading", *J. Soc. Naval Arch Japan* **168** (1990), 449–462.

Received 19 Jun 2017. Revised 11 Nov 2017. Accepted 29 Jan 2018.

JUNLIN DENG: junlin.deng@163.com
School of Transportation, Wuhan University of Technology, Heping street #1178, Wuchang District, Wuhan, 430063, China

PING YANG: pyangwhut@163.com
School of Transportation, Wuhan University of Technology, Heping street #1178, Wuchang District, Wuhan, 430063, China

YUAN CHEN: yuanc0801@163.com
School of Transportation, Wuhan University of Technology, Heping street #1178, Wuchang District, Wuhan, 430063, China

JIN HAN: wulihanjin@163.com
School of Transportation, Wuhan University of Technology, Heping street #1178, Wuchang District, Wuhan, 430063, China